# Comparative Assessment of PV Energy Forecasting Tools using Empirical Data from a Plant in Northeast Brazil

**Marcos Camargo Lima Filho[1], Pedro José dos Santos Neto[1], Juan Carlos Colque Ccarita[2], João Pedro C. Silveira[2], Diego Lucas de C. Martinez[3] and Tárcio André dos Santos Barros[2]**

[1] Power Electrotonics Laboratory (LEPO), School of Mechanical Engineering (FEM), Department of Integrated Systems (DSI), *Universidade Estadual de Campinas* (Unicamp), Campinas (Brazil)

[2] Power Electrotonics Laboratory (LEPO), School of Electrical and Computer Engineering (FEEC), *Universidade Estadual de Campinas* (Unicamp), Campinas (Brazil)

[3] Power Electrotonics Laboratory (LEPO), *Centro de Estudos de Energia e* Petróleo (CEPETRO), *Universidade Estadual de Campinas* (Unicamp), Campinas (Brazil)

**Abstract**

This study presents an evaluation of photovoltaic energy forecasting tools through a 24-month empirical analysis of a 36.3 kWp solar power plant in Northeast Brazil. The plant operated continuously from May 2023 to April 2025, with 99.59% availability. Using computational tools, PVsyst simulations and Solcast satellite-based data analyses were compared with real generation data, system's performance was evaluated using MAE, RMSE, and MAPE metrics. PVsyst was configured with site-specific parameters and loss modeling; Solcast data were processed via a data-mining workflow using module efficiency of 21.3% and loss assumptions comparable to PVsyst. PVsyst more closely matched observations (MAE 292.7 kWh/month; RMSE 403.15 kWh/month) than Solcast (MAE 355.16 kWh/month; RMSE 495.44 kWh/month). The results demonstrate PVsyst's superior accuracy (6.18%), attributed to its detailed system loss modeling, although it is a paid service. In contrast, Solcast data analyses showed a small difference (7.24%) and offers a viable open-access alternative for research. The findings reveal that, while PVsyst remains one of the widely used tools for technical designs, Solcast's database provides sufficient accuracy for feasibility studies when using a data mining algorithm to extract specific information complemented by equipment datasheets for forecasting the energy generation of the PV system. This contribution is a rigorously monitored agricultural case in Brazil's Northeast with a side-by-side comparison of a design-grade simulator and a satellite-based dataset.

*Keywords: Photovoltaic Energy Forecasting, PVsyst, Solcast, Empirical Performance Data*

## 1. Introduction

The growing demand for renewable energy has driven the development of grid-connected photovoltaic (PV) systems. Software tools such as PVsyst and SolarPlus play a crucial role in system design and performance simulation, providing generation estimates based on historical irradiance data, and technical losses, it is widely used in the design phase of PV systems, and its validation with real operational data under diverse climatic conditions and technical configurations is essential to ensure forecast accuracy on the other hand platforms like Solcast, which provide solar data through satellite imagery and atmospheric models, play a crucial role in simulations, with accuracy varying by region and seasonal factors. (Sarkis et al., 2024)

Solcast uses geostationary weather satellite imagery and numerical weather prediction models to generate data updated every five minutes. Several studies show that this data, validated against ground-based measurements, demonstrates high accuracy under various weather conditions (Zhang et al., 2024; Sayed, 2024).


10.18086/swc.2025.04.13 Available at http://proceedings.ises.org

Recent studies have examined the link between photovoltaic simulations and real energy generation data. Zhang et al. (2024) evaluated methods using monthly Global Horizontal Irradiance (GHI) averages to estimate Direct Normal Irradiance (DNI) and Diffuse Horizontal Irradiance (DHI), comparing NASA data with Baseline Surface Radiation Network measurements. Authors stressed the importance of validating theoretical models with local data. In large-scale applications like green hydrogen plants, emphasized the real solar irradiance needed data to ensure accurate generation capacity and viability. (Zhang et al., 2024; Bhang et al. 2023).

Sarkis et al. (2024) validated GHI forecasts using public cameras and deep neural networks, achieving results similar Solcast without satellite data. Gonzalez and Martins (2024) analyzed a PV system, validating SOLergo simulations with real data, Global Tilted Irradiance (GTI), and highlighting the need for regional model calibration in humid, seasonally variable areas. (Bhang et al., 2023; Sarkis et al., 2024; Gonzalez and Martins, 2024; Zhang et al., 2024).

Following this line of investigation this study presents an empirical comparison between PVsyst simulations and Solcast historical data analyses, based on two years of real-world operation, evaluating forecast accuracy for PV systems. The power plant was monitored from May 2023 to April 2025. The system consists of sixty-six solar modules of 550W and a DC-AC inverter of 36 kWp, that was installed on a coconut production farm in the city of Acaraú, in the state of Ceará, located in the northeastern region of Brazil, as in section 2.

## 2. Literature Review and Related Works

Recent research has brought photovoltaic simulations closer to real generation data, underscoring why empirical validation is crucial for improving forecast reliability and informing solar system design. Sarkis et al. (2024) demonstrated that global horizontal irradiance can be predicted on an intraday horizon using public webcam images combined with a CNN-LSTM architecture. Notably, the performance was comparable to commercial services even without satellite imagery or full numerical weather models, opening avenues for low-cost solutions based on local visual sensors with limited access to high-resolution meteorological data (Sarkis et al., 2024).

In a complementary direction, Zhang et al. (2024) compared satellite-derived products based on Clouds and the Earth's Radiant Energy System (CERES) with reference measurements from the Baseline Surface Radiation Network (BSRN). The authors showed that, although GHI exhibits good agreement, DHI and DNI contain biases that can be corrected to improve practical use. After correction, the dataset enabled more accurate GTI and hourly global tracking relative to surface observations. The central message is clear: remote data, however sophisticated, requires local calibration to avoid systematic errors in production estimates (Zhang et al., 2024).

The need for validation spans multiple scales and configurations. For non-conventional arrays, recent literature reports meaningful gains when orientation and thermal context are modeled accurately. Carrera et al. (2023) analyzed an east–west system at a hotel using PVsyst and reported a performance ratio of 0.80, higher energy yield per unit area, and lower average operating temperature compared with a conventional south-facing layout. (Carrera et al. 2023)

On aquatic platforms, Osama et al. (2024) experimentally evaluated a bifacial floating east–west system in Catania, validating models in PVsyst and SAM. When loss assumptions were harmonized, both tools produced comparable results, with a slight advantage for PVsyst under varying radiative and thermal conditions (Osama et al., 2024).

In residential and off-grid contexts, the literature has also proposed hybrid sizing methodologies that combine design intuition with numerical calculation, reducing computational effort without sacrificing robustness. For example, Abed et al. (2025) describe an initial exploration workflow using Global Solar Atlas data and PVsyst reports, followed by rigorous validation with electromagnetic models and real measurements, prioritizing the “critical month” to accelerate simulations while maintaining technical fidelity (Abed et al., 2025).

Gonzalez and Martins (2024) studied a 3.3 kWp system on Brazil’s southeastern coast, a humid region with substantial aerosol loading, and found that actual generation exceeded the prediction of a numerical tool by up to

10%. They attributed this deviation to atypical climatic conditions during the measurement period and emphasized the importance of local data for model calibration (Gonzalez & Martins, 2024).

Taken together, these studies converge on three points. First, tools such as PVsyst and SAM, as well as satellite services like Solcast and NASA/CERES, are valuable but require bias corrections and careful loss modeling, including soiling, temperature, cabling, and inverters, along with appropriate representation of tilt, azimuth, bifaciality, and mounting type. Carrera et al. (2023) and Osama et al. (2024) highlight practical gains when array geometry and losses are modeled realistically, including in east–west and floating systems. Second, corrections and calibration using local measurements substantially improve the accuracy of satellite-derived data, as argued by Zhang et al. (2024). Third, project workflows that integrate climatic pre-analysis, detailed simulation, and field validation, as in Abed et al. (2025), make the process more efficient without compromising technical quality (Carrera et al., 2023; Osama et al., 2024; Zhang et al., 2024; Abed et al. 2025).

A relevant gap remains regarding long-term empirical series in agricultural environments in Brazil's Northeast, featuring side-by-side comparisons between PVsyst-based projections and satellite service forecasts or historical datasets, such as Solcast, for the same grid-connected system.

The present study addresses this gap by monitoring a 36.3 kWp plant for 24 months at a green-coconut farm in Ceará, Brazil. Where the system achieved 99.59% availability. We provide a coherent comparison between PVsyst and Solcast historical data processed via a data-mining algorithm, both aligned to the same geographic measurements. This strategy, consistent with the evidence reported by Gonzalez and Martins (2024), Osama et al. (2024), Carrera et al. (2023), Sarkis et al. (2024), and Zhang et al. (2024), reinforces that the combination of detailed simulation, satellite historical databases, and systematic field validation is a viable pathway to reduce forecasting errors and improve techno-economic feasibility analyses for photovoltaic projects.

## 3. Objective and Methodology

The main objective is to compare PVsyst-simulated energy-generation estimates with Solcast forecasts and evaluate both against the actual monthly production of a grid-connected PV system monitored over two years (May 2023 to April 2025) on a coconut-producing farm in Acaraú, Ceará, Brazil.

For the comparative analysis, statistical methods were applied to monthly-aggregated data across the entire monitoring period. The data sources include:

(i) PVsyst simulation based on the system's technical configuration;

(ii) Solar irradiance and generation forecasts from the Solcast platform, with Figure 1 shown Algorithm to Processing Solcast Data that was used to process the raw database;

(iii) Real generation data collected from the installed PV system and retrieved from the Growatt cloud service database over two years.

To evaluate the accuracy of simulated and forecasted values, the following statistical metrics were used: Mean Absolute Error (MAE) in eq.1, Root Mean Square Error (RMSE) in eq.2, and Mean Absolute Percentage Error (MAPE) in eq.3, which are widely adopted in the literature for model performance assessment (Wilks, 2019).

$$MAE = \frac{1}{n}\sum_{i=1}^{n}|y_i - \hat{y}_i| \quad \text{(eq. 1)}$$

$$RMSE = \sqrt{\frac{1}{n}\sum_{i=1}^{n}(y_i - \hat{y}_i)^2} \quad \text{(eq. 2)}$$

$$MAPE = \frac{100\%}{n}\sum_{i=1}^{n}\frac{|y_i - \hat{y}_i|}{y_i} \quad \text{(eq. 3)}$$

where:

$n$ is number of observations.
$y_i$ is the actual (observed) value at index $i$.
$\hat{y}i$ is the predicted (estimated) value at index $i$.
$| y_i - \hat{y}i |$ denotes the absolute error between the actual and predicted values.

Accordingly, the methodology consists of a statistical comparison of three datasets. Because every PV installation requires a commercial yield estimate for sales and a detailed design for deployment, PVsyst, the most used project-design software, was adopted to provide simulation outputs.

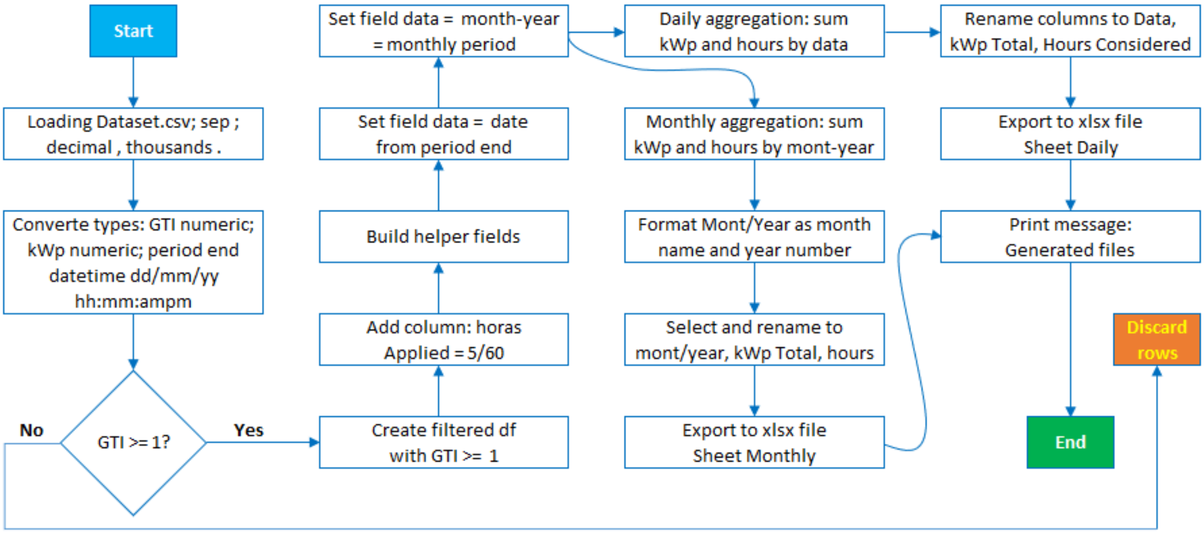


**Fig. 2: Flowchart of the MATLAB algorithm used to process Solcast solar data**

The satellite data was obtained from Solcast, which is widely used in academic research. To evaluate this model and satellite estimates for the region, the "theoretical" values are compared with in-field measurements collected from a grid-connected photovoltaic system installed on a coconut farm and operated continuously on period.

## 4. Project and Development

The support structure for the PV modules, shown in Figure 3, was constructed using reinforced concrete columns and sealed wooden beams. DC cables were routed through 2-inch polymer conduits to the PV modules to solar inverter, in accordance with ABNT NBR standards, shown in Figure 2.


**Fig. 2: Installation of 2-inch polymer conduits (left) and DC/AC solar inverter (right) [Authors]**

The modules were installed with an 8° tilt and oriented toward true north, shown in Figure 3. Beam spacing followed module specifications and construction requirements. The completed installation assembly (operational PV modules), shown in Figure 3.

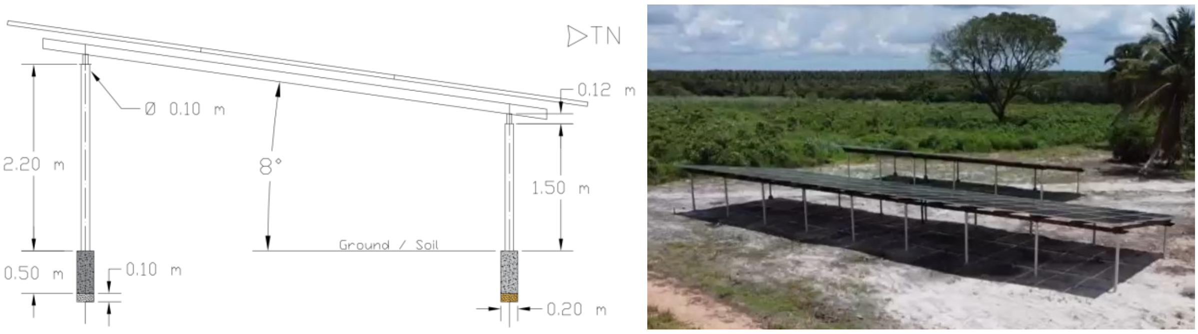


**Fig. 3: View of the project structure (left) and the completed photovoltaic installation (right) [Authors]**

The photovoltaic system comprises sixty-six PV modules (JAM72S30-550/MR, Trina Solar, 2023), each with a maximum power output of 550 W and efficiency up to 21.3%, and one inverter (Growatt MID 36KTL3-X, 2023), a three-phase unit with 98.8% maximum efficiency. This setup, shown in Figures 2-3, is installed on a coconut-producing farm, shown in Figure 4. The system generates electricity for grid injection, producing credits that power irrigation pumps across a 40-hectare coconut plantation.

**Fig. 4: Aerial view of the coconut farm, the image (right) showing the PV installation and solar panel layout [©2025 Google Maps]**

The PVsyst software was used for simulation, incorporating datasheet information from the modules and inverter, solar irradiance data from Meteonorm 8.2, system loss estimates, and site-specific parameters such as tilt and environmental conditions.

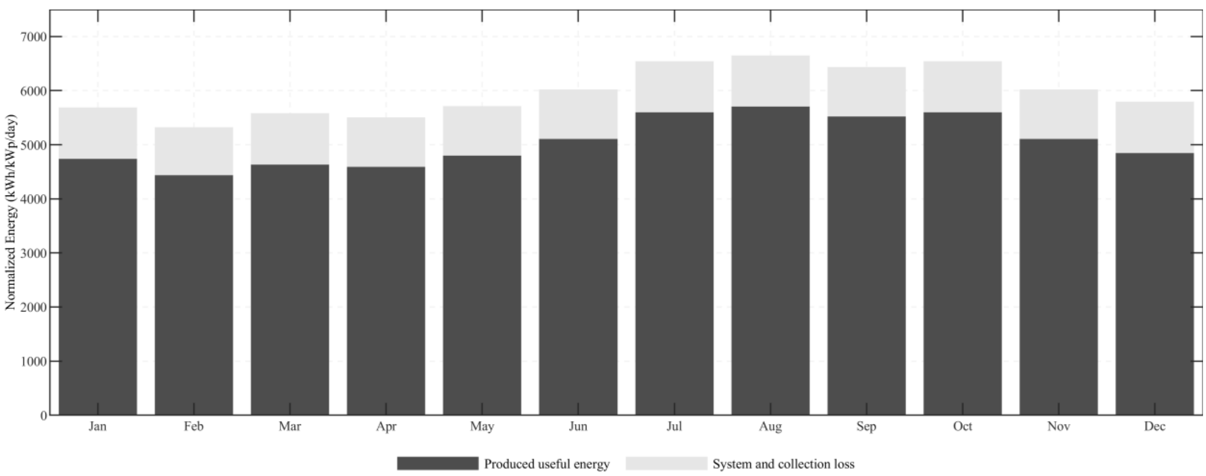


**Fig. 5: Projected Monthly Energy Output and Losses Calculated by the PVsyst Software for the PV System**

The software PVsyst also uses information about the module tilt and the environmental conditions of the specified installation site. In this way, it can calculate the energy generation projection and system losses, as shown above.

The chart, shown in Figure 6, was used to determine the module azimuth and tilt angle, verify the absence of structural shading during critical hours, and size the minimum inter-row spacing. The curves depict the apparent solar path throughout the year, and the dashed concentric circles indicate solar elevation.

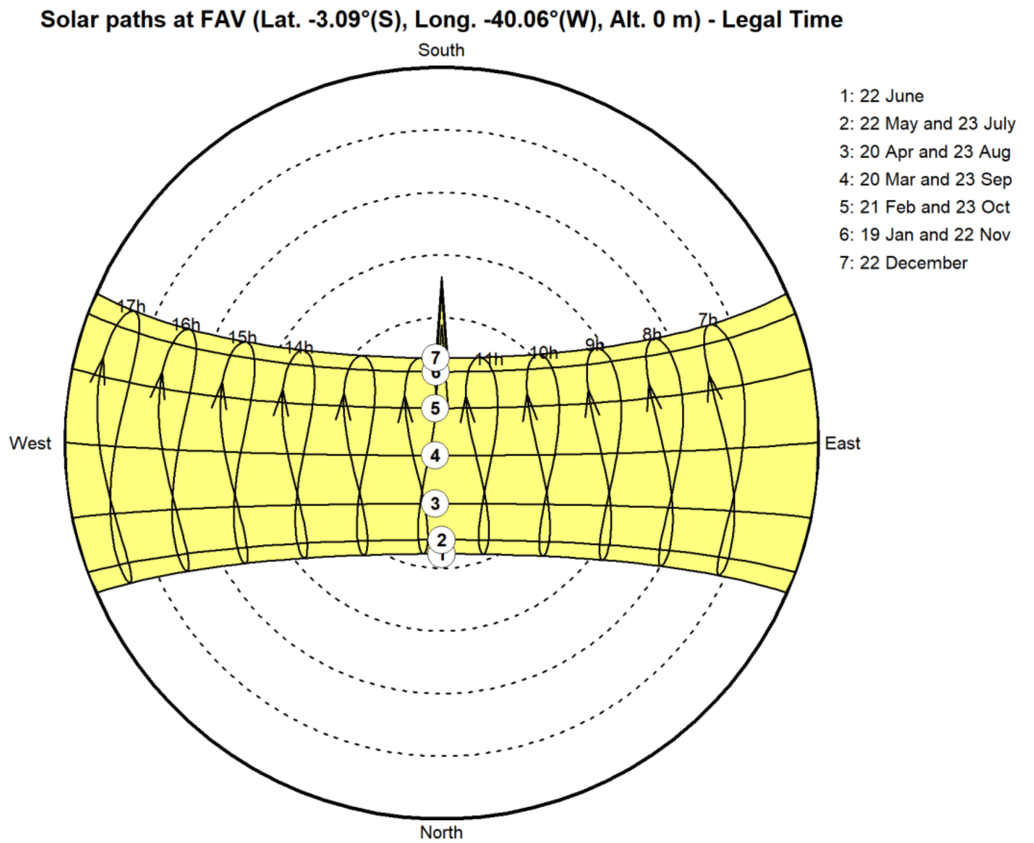


**Fig. 6: Sun-path chart and solar-hour lines [PVsyst v7 (PVsyst SA, 2025)]**

The chart also confirms the seasonal reversal of the noon incidence side: the Sun is to the north during the Austral autumn and winter and to the south in summer, which is important for assessing gains and losses under a single fixed tilt over the year and for interpreting seasonal variations in GTI in the simulations.

Data from the same period must be obtained using the Solcast service, shown in Figure 7, which provides global coverage and offers data for virtually any location on Earth. This database is a comprehensive resource for solar irradiance data and forecasting, widely used in research and applications in the field of solar energy.

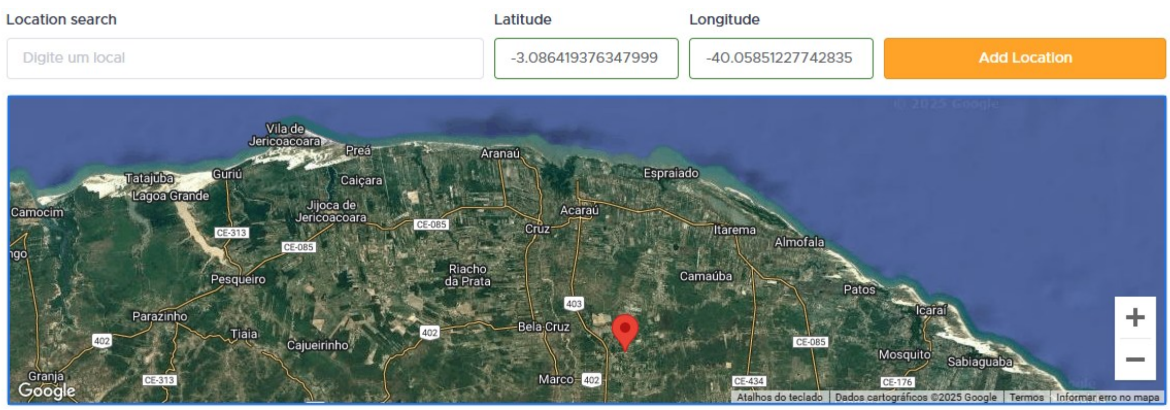


**Fig. 7: Geographic location (GPS) of solar data collected from Solcast [Solcast Pty Ltd, 2025]**

## 5. Results and Discussion

Table 1 presents the data datasets: PVsyst simulation values adjusted for system losses, shown in Figure 8; Solcast historical data calculated using a 21.3% module efficiency (datasheet), shown in Figure 9, similar loss assumptions as in PVsyst, and using the data mining algorithm to process the database to extract the GTI per day and accumulated month. In the same table has the real energy injected into the grid-connected over two years, accounting for all losses such as inverter conversion, cabling, and soiling, shown in Figure 10.

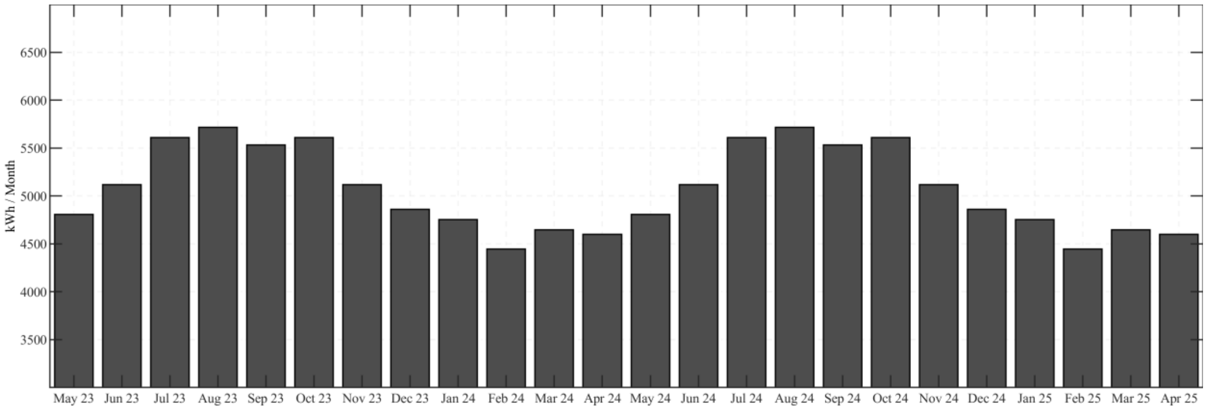


**Fig. 8: Database from PVsyst by Meteonorm data**

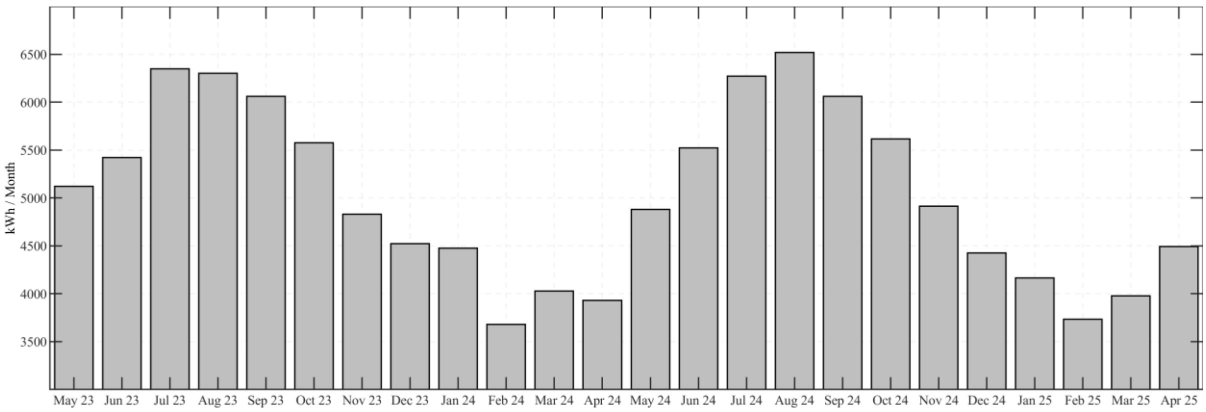


**Fig. 9: Database from Solcast after data mining and PV module efficiency applied with the algorithm Matlab**

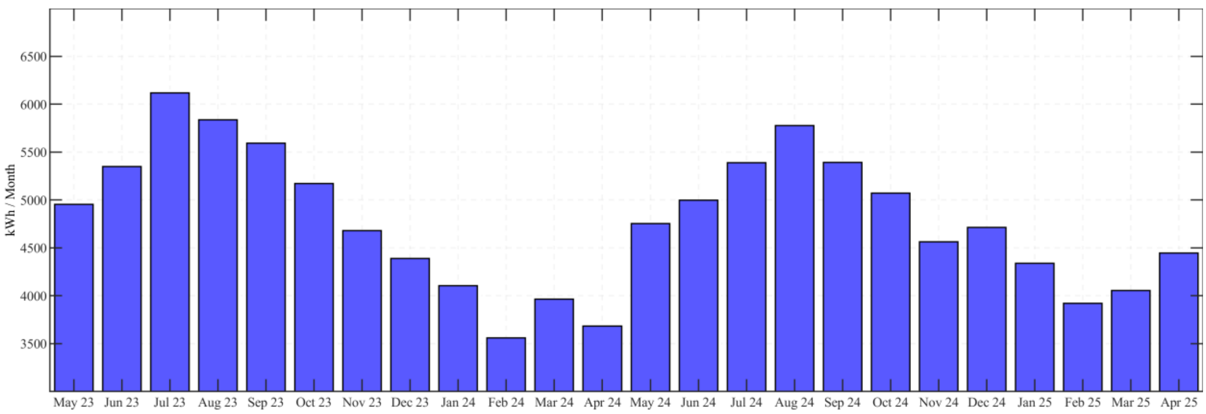


**Fig. 10: Database from cloud Growatt storage**

The monthly net energy generation was obtained from Growatt's cloud platform for the period May 2023 to April 2025. The photovoltaic system achieved 99.59% operational availability. Data was accessed via the customer portal (https://server.growatt.com), which provides complete repository access for the installed system.

The comparison of monthly energy generation from three sources, measured production, and PVsyst simulations, and Solcast forecasts, was performed by computing absolute errors and summary performance metrics (Table 1); the corresponding time-series curves are presented in Figure 11.

**Tab. 1: Dataset of Real PV system, Software PVsyst, and Dataset of Solcast**

| Month | Generated by real PV system | PVsyst Projected | | Solcast (satellite data) | |
|---|---|---|---|---|---|
| | | Database | Absolute error | Database | Absolute error |
| 1 | 4953,7 | 4807,7 | 146,0 | 5122,4 | 168,7 |
| 2 | 5348,5 | 5118,5 | 230,0 | 5423,2 | 74,7 |
| 3 | 6118,0 | 5610,3 | 507,7 | 6349,2 | 231,2 |
| 4 | 5839,3 | 5717,4 | 121,9 | 6304,2 | 464,9 |
| 5 | 5594,2 | 5533,0 | 61,2 | 6061,6 | 467,4 |
| 6 | 5172,6 | 5610,3 | 437,7 | 5577,3 | 404,7 |
| 7 | 4680,1 | 5118,5 | 438,4 | 4829,9 | 149,8 |
| 8 | 4390,1 | 4860,9 | 470,8 | 4522,2 | 132,1 |
| 9 | 4106,2 | 4753,8 | 647,6 | 4475,2 | 369,0 |
| 10 | 3559,1 | 4447,1 | 888,0 | 3681,2 | 122,1 |
| 11 | 3964,3 | 4646,7 | 682,4 | 4029,5 | 65,2 |
| 12 | 3684,3 | 4600,5 | 916,2 | 3931,4 | 247,1 |
| 13 | 4755,2 | 4807,7 | 52,5 | 4881,5 | 126,3 |
| 14 | 4999,7 | 5118,5 | 118,8 | 5523,6 | 523,9 |
| 15 | 5390,7 | 5610,3 | 219,6 | 6273,8 | 883,1 |
| 16 | 5777,9 | 5717,4 | 60,5 | 6521,2 | 743,3 |
| 17 | 5391,8 | 5533,0 | 141,2 | 6062,6 | 670,8 |
| 18 | 5071,8 | 5610,3 | 538,5 | 5617,3 | 545,5 |
| 19 | 4564,6 | 5118,5 | 553,9 | 4914,3 | 349,7 |
| 20 | 4714,0 | 4860,9 | 146,9 | 4425,3 | 288,7 |
| 21 | 4340,9 | 4753,8 | 412,9 | 4165,8 | 175,1 |
| 22 | 3922,3 | 4447,1 | 524,8 | 3735,3 | 187,0 |
| 23 | 4055,5 | 4646,7 | 591,2 | 3979,0 | 76,5 |
| 24 | 4446,8 | 4600,5 | 153,7 | 4494,2 | 47,4 |

Applying equations 1, 2, and 3, and these results are summarized in Table 2, which compares the simulated values and their deviations from real monthly generation database.

**Tab. 2: The MAE, RMSE, and MAPE metrics were calculated**

| Accuracy Evaluation Methods | PVsyst (kWh/Month) | Solcast (kWh/Month) |
|---|---|---|
| MAE | 292.73 | 355.16 |
| RMSE | 403.15 | 495.44 |
| MAPE (%) | 6.18 | 7.24 |

The 1.06% MAPE difference between PVsyst and Solcast is attributable to indirect losses such as DC/AC cabling and inverter conversion, among others. Although datasheet parameters were applied, show in Figures 12 and 13, these additional losses can account for the observed discrepancy. The 6.18% MAPE difference between PVsyst and the installed system reflects real operating effects, notably module soiling. During the period, only one cleaning event was performed, approximately 18 months after commissioning, which reduced soiling relative to the constant-loss assumptions (from December 2024 onward). A similar pattern is observed from commissioning until roughly five months, when the measured production begins to fall below the projections.

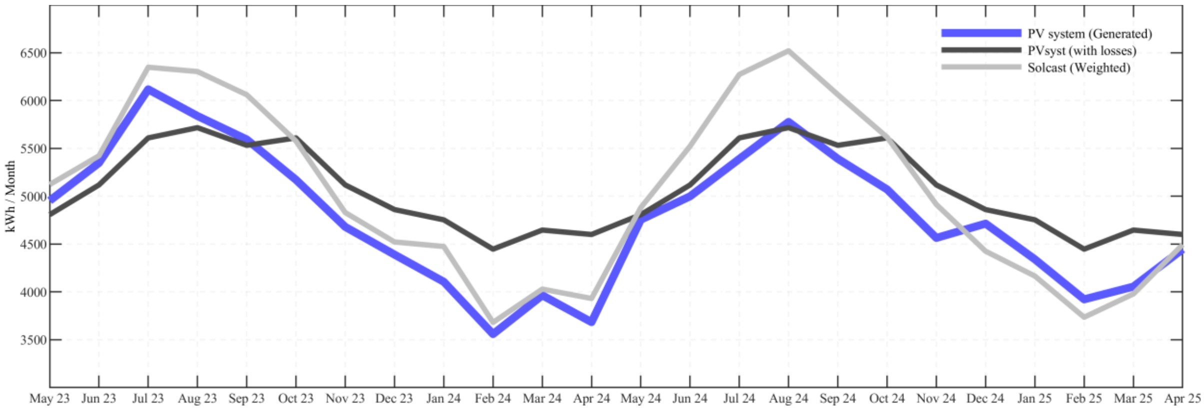


**Fig. 11: Dataset comparisons: Real generation data versus PVsyst projection data versus Solcast historical data**

## 6. Conclusion

The comparison of 24 months of real operation (from May 2023 to April 2025) with PVsyst projections and Solcast historical data for a grid-connected photovoltaic system (36 kWp; 66 × 550 W) on the coast of Ceará shows that PVsyst more closely matched the measured data (MAE 292.7 kWh/month; MAPE 6.18%) than Solcast (MAE 355.2 kWh/month; MAPE 7.24%), corresponding to approximately 17.6% lower MAE and 14.6% lower MAPE.

When calibrated with site-specific losses and parameters, PVsyst provides more accurate estimates for humid, seasonally variable contexts such as Brazil's northeastern coast. In this study, Solcast was parameterized with a module efficiency of 21.3% and losses similar to those used in PVsyst. It preserved temporal coherence and broad geographic coverage but exhibited a tendency to overestimate in several months, indicating a seasonal bias that warrants regional adjustment.

From a practical standpoint, detailed simulation with PVsyst should be combined with satellite-based datasets from Solcast, validated against local measurements, and embedded in a continuous calibration loop that incorporates operational data (for example, 99.59% availability), realized losses, and seasonal effects. For investment return projections, the expected performance degradation reported in the module datasheet should be incorporated at annual or multi-year cycles. Historical irradiance and production proxies from Solcast can then be used to project generation while explicitly accounting for system operational constraints and utility grid interruptions. Applying a conservative correction factor based on the maximum observed MAPE (7.25%) would further align projections with realized generation. As shown in the results, this percentage difference suggests that PV modules in this region should be cleaned approximately every four months so that system efficiency remains closer to the ideal (projected) generation.

Future work should broaden the sample to additional agricultural regions and analyze higher temporal resolutions to refine models that capture soiling and potential shading effects, depending on the crop and local spacing. Such analyses would support evaluating seasonal adjustments to array tilt and azimuth to optimize performance.

## 7. Acknowledgments

This study was financed by TotalEnergies through the R&D incentive program of the Brazilian National Agency of Petroleum, Natural Gas and Biofuels (ANP) in partnership with CEPETRO and FEEC at UNICAMP.

We thank the Power Electronics Laboratory (LEPO), School of Electrical and Computer Engineering (FEEC), and the School of Mechanical Engineering (FEM) at UNICAMP for institutional and technical support.

We are also grateful to the staff of the VerdeAmarelo farm for their assistance during site visit and data collection.

## 8. References

Abed, M., Reddy, A., Jyothsna, T.R. and Mohammed, N., 2025. Optimal sizing and performance assessment of stand-alone photovoltaic systems using an optimum hybrid sizing strategy. Results in Engineering, [online] Article 103793. https://doi.org/10.1016/j.rineng.2024.103793

Bhang, B.G., Hyun, J.H., Ahn, S.-H. and Choi, J.H., 2023. Optimal design of bifacial floating photovoltaic system with different installation azimuths. IEEE Access, 11, pp.1456–1466. https://doi.org/10.1109/ACCESS.2022.3233100

Carrera, L.A.I., Silva, R.F. and Oliveira, M.C., 2023. Energy efficiency analysis of east–west oriented photovoltaic systems for buildings: A technical–economic–environmental approach. IEEE Access, 11, pp.137660–137679. https://doi.org/10.1109/ACCESS.2023.3340145

Gonzalez, J.O. and Martins, F.R., 2024. Performance study of a photovoltaic system operating on the southeastern coast of Brazil. IEEE Latin America Transactions, 22(5), pp.410–416. Available at: https://latamt.ieeer9.org/index.php/transactions/article/view/8256 [Accessed Feb. 2025].

Google (maps) Google Maps. [online] Available at: https://www.google.com/maps [Accessed 21 Oct. 2025].

Growatt, 2022. MID 10–40KTL3-X – User Manual (includes MID 36KTL3-X). [online] Available at: https://growatt.tech/wp-content/uploads/shared-files/MID-10-40KTL3-X-User-Manual-EN-202202.pdf [Accessed Feb. 2025].

JA Solar, 2021. JAM72S30-525/550 MR – Photovoltaic module datasheet. [online] Available at: https://www.jasolar.com/uploadfile/2021/0706/20210706053524693.pdf [Accessed Jan. 2025].

Kosmopoulos, P., 2024. Management of the Sun's power in real-time. In: P. Kosmopoulos, ed., Planning and Management of Solar Power from Space. London and San Diego: Academic Press, pp.121–139. https://doi.org/10.1016/B978-0-12-823390-0.00003-X

PVsyst SA, 2023. PVsyst 7 – Grid-connected systems: My first project. [online] Available at: https://www.pvsyst.com/pdf/pdf-tutorials/.../pvsyst-tutorial-v7-grid-connected-1-en.pdf [Accessed Feb. 2025].

PVsyst SA, 2024. PVsyst 7 – Grid connected systems: Meteo data handling. [online] Available at: https://www.pvsyst.com/pdf/pdf-tutorials/.../pvsyst-tutorial-v7-grid-connected-3-en.pdf [Accessed Mar. 2025].

PVsyst SA, 2020. Importing data from Meteonorm Program. [online] Available at: https://www.pvsyst.com/help/meteo-database/import-meteo-data/meteonorm-data-and-program/importing-data-from-meteonorm-program.html [Accessed Feb. 2025].

Sayed, K., Elsayed, M.M. and Mohamed, A., 2025. Feasibility and economic assessment of a PV–wind hybrid charging station in the Bronx, NY. IEEE Access, 13. Available at: https://smartgrid.ccny.cuny.edu/publication/ [Accessed Mar. 2025].

Sarkis, R., Oguz, I., Psaltis, D., Paolone, M., Moser, C. and Lambertini, L., 2024. Intraday solar irradiance forecasting using public cameras. Solar Energy, 275, Article 112600. https://doi.org/10.1016/j.solener.2024.112600

Solcast (time-series) Solcast. [online] Available at: https://solcast.com/ [Accessed Jan. 2025].

Wilks, D.S., 2019. Statistical Methods in the Atmospheric Sciences. 4th ed. Amsterdam: Elsevier. ISBN 9780128158234.

Zhang, T., Li, X., Wang, Y., et al., 2024. Validation of monthly-mean-based beam irradiance methods using ground measurements. Solar Energy, 274, Article 112538. https://doi.org/10.1016/j.solener.2024.112538

Zidane, T.E.K., Aziz, A.S., Zahraoui, Y., et al., 2023. Grid-connected solar PV power plants optimization: A review. IEEE Access, 11, pp.108754–108771. https://doi.org/10.1109/ACCESS.2023.3299815

# Appendix: PV module Datasheet

JA SOLAR — JAM72S30 525-550/MR/1500V Series

## MECHANICAL DIAGRAMS

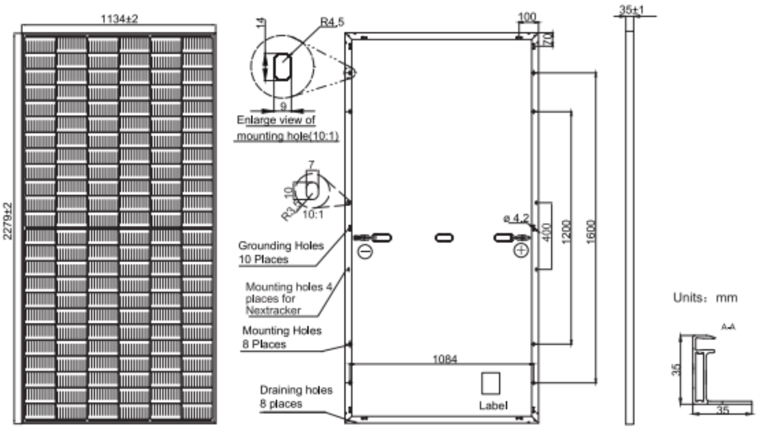


Remark: customized frame color and cable length available upon request

## SPECIFICATIONS

| | |
|---|---|
| Cell | Mono |
| Weight | 28.6kg±3% |
| Dimensions | 2279±2mm×1134±2mm×35±1mm |
| Cable Cross Section Size | 4mm²（IEC）, 12 AWG(UL) |
| No. of cells | 144(6×24) |
| Junction Box | IP68, 3 diodes |
| Connector | Genuine MC4-EVO2<br>QC 4.10-35/45 |
| Cable Length (Including Connector) | Portrait: 300mm(+)/400mm(-);<br>Landscape: 1300mm(+)/1300mm(-) |
| Country of Manufacturer | China/Vietnam |

## ELECTRICAL PARAMETERS AT STC

| TYPE | JAM72S30 -525/MR/1500V | JAM72S30 -530/MR/1500V | JAM72S30 -535/MR/1500V | JAM72S30 -540/MR/1500V | JAM72S30 -545/MR/1500V | JAM72S30 -550/MR/1500V |
|---|---|---|---|---|---|---|
| Rated Maximum Power(Pmax) [W] | 525 | 530 | 535 | 540 | 545 | 550 |
| Open Circuit Voltage(Voc) [V] | 49.15 | 49.30 | 49.45 | 49.60 | 49.75 | 49.90 |
| Maximum Power Voltage(Vmp) [V] | 41.15 | 41.31 | 41.47 | 41.64 | 41.80 | 41.96 |
| Short Circuit Current(Isc) [A] | 13.65 | 13.72 | 13.79 | 13.86 | 13.93 | 14.00 |
| Maximum Power Current(Imp) [A] | 12.76 | 12.83 | 12.90 | 12.97 | 13.04 | 13.11 |
| Module Efficiency [%] | 20.3 | 20.5 | 20.7 | 20.9 | 21.1 | 21.3 |
| Power Tolerance | 0~+5W | | | | | |
| Temperature Coefficient of Isc(α_Isc) | +0.045%/°C | | | | | |
| Temperature Coefficient of Voc(β_Voc) | -0.275%/°C | | | | | |
| Temperature Coefficient of Pmax(γ_Pmp) | -0.350%/°C | | | | | |
| STC | Irradiance 1000W/m², cell temperature 25°C, AM1.5G | | | | | |

Remark: Electrical data in this catalog do not refer to a single module and they are not part of the offer.They only serve for comparison among different module types.
Measurement tolerance at STC: Pmax ±3 %, Voc ±3% and Isc ±4%.

## ELECTRICAL PARAMETERS AT NOCT

| TYPE | JAM72S30-525 /MR/1500V | JAM72S30-530 /MR/1500V | JAM72S30-535 /MR/1500V | JAM72S30-540 /MR/1500V | JAM72S30-545 /MR/1500V | JAM72S30-550 /MR/1500V |
|---|---|---|---|---|---|---|
| Rated Max Power(Pmax) [W] | 397 | 401 | 405 | 408 | 412 | 416 |
| Open Circuit Voltage(Voc) [V] | 46.05 | 46.18 | 46.31 | 46.43 | 46.55 | 46.68 |
| Max Power Voltage(Vmp) [V] | 38.36 | 38.57 | 38.78 | 38.99 | 39.20 | 39.43 |
| Short Circuit Current(Isc) [A] | 10.97 | 11.01 | 11.05 | 11.09 | 11.13 | 11.17 |
| Max Power Current(Imp) [A] | 10.35 | 10.39 | 10.43 | 10.47 | 10.51 | 10.55 |
| NOCT | Irradiance 800W/m², ambient temperature 20°C,wind speed 1m/s, AM1.5G | | | | | |

## OPERATING CONDITIONS

| | |
|---|---|
| Maximum System Voltage | 1500V DC (IEC) |
| Operating Temperature | -40℃~+85℃ |
| Maximum Series Fuse Rating | 25A |
| Maximum Static Load,Front*<br>Maximum Static Load,Back* | 3600Pa, 1.5<br>1600Pa, 1.5 |
| NOCT | 45±2℃ |
| Safety Class | Class Ⅱ |
| Fire Performance | UL Type 1 |

*For NexTracker installations, Maximum Static Load, Front is 2000Pa while Maximum Static Load, Back is2000Pa.

## CHARACTERISTICS

Current-Voltage Curve JAM72S30-540/MR/1500V

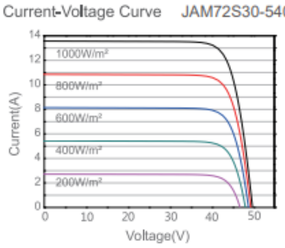


Power-Voltage Curve JAM72S30-540/MR/1500V

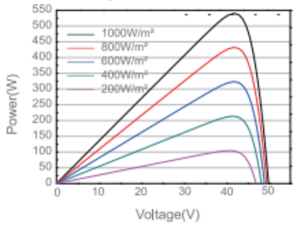


Current-Voltage Curve JAM72S30-540/MR/1500V

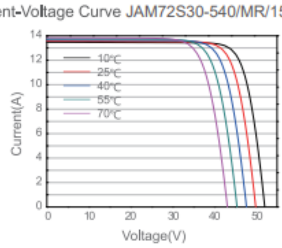


**Premium Cells, Premium Modules** Version No.: Global_EN_20210607A

**Fig. 12: Datasheet for the JAM72S30-series photovoltaic module**

# Appendix: Solar Inverter (DC–AC) Datasheet

| Datasheet | MID 25KTL3-X1 | MID 30KTL3-X | MID 33KTL3-X | MID 36KTL3-X | MID 40KTL3-X |
|---|---|---|---|---|---|
| **Input data (DC)** | | | | | |
| Max. recommended PV power (for module STC) | 37500W | 45000W | 49500W | 54000W | 60000W |
| Max. DC voltage | 1100V | | | | |
| Start Voltage | 250V | | | | |
| Normal Voltage | 600V | | | | |
| MPPT voltage range | 200-1000V | | | | |
| No. of MPP trackers | 3 | 3 | 3 | 4 | 4 |
| No. of PV strings per MPP tracker | 2 | | | | |
| Max.input current per MPP tracker | 26A | | | | |
| Max. short-circuit current per MPP tracker | 32A | | | | |
| **Output data (AC)** | | | | | |
| AC nominal power | 25000W | 30000W | 33000W | 36000W | 40000W |
| Max. AC apparent power | 27700VA | 33300VA | 36600VA | 39600VA | 44000VA |
| Nominal AC voltage (range*) | 220V/380V, 230V/400V (340-440V) | | | | |
| AC grid frequency (range*) | 50/60 Hz (45-55Hz/55-65 Hz) | | | | |
| Max. output current | 41.9A | 50.5A | 55.5A | 60.0A | 66.6A |
| Adjustable power factor | 0.8leading…0.8lagging | | | | |
| THDi | <3% | | | | |
| AC grid connection type | 3W+N+PE | | | | |
| **Efficiency** | | | | | |
| Max.efficiency | 98.8% | | | | |
| European efficiency | 98.5% | | | | |
| MPPT efficiency | 99.9% | | | | |
| **Protection devices** | | | | | |
| DC reverse polarity protection | Yes | | | | |
| DC Switch | Yes | | | | |
| AC/DC surge protection | Type II / Type II | | | | |
| Insulation resistance monitoring | Yes | | | | |
| AC short-circuit protection | Yes | | | | |
| Ground fault monitoring | Yes | | | | |
| Grid monitoring | Yes | | | | |
| Anti-islanding protection | Yes | | | | |
| Residual-current monitoring unit | Yes | | | | |
| String monitoring | Yes | | | | |
| AFCI protection | Yes* | | | | |
| **General data** | | | | | |
| Dimensions (W / H / D) | 580/435/230mm | | | | |
| Weight | 29.5kg | 29.5kg | 29.5kg | 30.5kg | 30.5kg |
| Operating temperature range | - 25°C ... +60°C | | | | |
| Nighttime power consumption | < 1W | | | | |
| Topology | Transformerless | | | | |
| Cooling | Smart air cooling | | | | |
| Protection degree | IP66 | | | | |
| Relative humidity | 0-100% | | | | |
| Altitude | 4000m | | | | |
| DC connection | H4/MC4(Optional) | | | | |
| AC connection | Cable gland+OT terminal | | | | |
| Display | OLED+LED/WIFI+APP | | | | |
| Interfaces: RS485 / USB / WIFI/ GPRS / RF/ LAN | Yes/Yes/Optional/Optional/Optional/Optional | | | | |
| Warranty: 5 years / 10 years | Yes/Optional | | | | |
| CE, VDE0126, Greece, EN50549, C10/C11, UTE C 15-712, IEC62116,IEC61727, IEC 60068, IEC 61683, CEI0-21, CEI0-16, N4105, TOR Erzeuger, G98/G99, G100, AS/NZS 3100, AS4777, UNE217001, UNE206007, PO12.2, KSC8565 | | | | | |

* The AC voltage range and frequency range may vary depending on specific country grid standard. All specifications are subject to change without notice.
* AFCI function need to be activated after installation.

**SHENZHEN GROWATT NEW ENERGY CO.,LTD.** A: 4-13/F,Building A,Sino-German(Europe)Industrial Park,Hangcheng Ave,Bao'an District,Shenzhen,China
T: + 86 755 2747 1900 F: + 86 755 2749 1460 E: info@ginverter.com

**Fig. 13: Datasheet for the Growatt-series solar inverter**